Metabolic Engineering 66 (2021) 167–178

Contents lists available at ScienceDirect

Metabolic Engineering

journal homepage: www.elsevier.com/locate/meteng

Towards bio-upcycling of polyethylene terephthalate

Till Tiso [a,1], Tanja Narancic [b,c,1], Ren Wei [d,2], Eric Pollet [e], Niall Beagan [b], Katja Schröder [a], Annett Honak [d], Mengying Jiang [e,h], Shane T. Kenny [f], Nick Wierckx [a,g], Rémi Perrin [h], Luc Avérous [e], Wolfgang Zimmermann [d], Kevin O'Connor [b,c,**], Lars M. Blank [a,*]

[a] iAMB - Institute of Applied Microbiology. ABBt - Aachen Biology and Biotechnology, RWTH Aachen University, Worringerweg 1, D-52074, Aachen, Germany
[b] BiOrbic - SFI Bioeconomy Research Centre, University College Dublin, Belfield, Dublin 4, Ireland
[c] School of Biomolecular and Biomedical Science and UCD Earth Institute, University College Dublin, Belfield, Dublin 4, Ireland
[d] Department of Microbiology and Bioprocess Technology, Institute of Biochemistry, Leipzig University, Johannisallee 23, D-04103, Leipzig, Germany
[e] BioTeam/ICPEES-ECPM, UMR CNRS 7515, Strasbourg University, 25 rue Becquerel, F-67087, Strasbourg Cedex 2, France
[f] Bioplastech Ltd., NovaUCD, Belfield Innovation Park, University College Dublin, Belfield, Dublin 4, Ireland
[g] Institute of Bio- and Geosciences IBG-1: Biotechnology, Forschungszentrum Jülich, 52425, Jülich, Germany
[h] SOPREMA, 14 rue de Saint-Nazaire, F-67025 Strasbourg Cedex, France

ARTICLE INFO

Dedicated to the memory of Shane T. Kenny, an early visionary of the plastic upcycling approach (1983–2020).

Keywords:
Polyethylene terephthalate (PET) degradation
Metabolic engineering
Biopolymers
Pseudomonas putida
Synthetic biology

ABSTRACT

Over 359 million tons of plastics were produced worldwide in 2018, with significant growth expected in the near future, resulting in the global challenge of end-of-life management. The recent identification of enzymes that degrade plastics previously considered non-biodegradable opens up opportunities to steer the plastic recycling industry into the realm of biotechnology.

Here, the sequential conversion of post-consumer polyethylene terephthalate (PET) into two types of bioplastics is presented: a medium chain-length polyhydroxyalkanoate (PHA) and a novel bio-based poly(amide urethane) (bio-PU). PET films are hydrolyzed by a thermostable polyester hydrolase yielding highly pure terephthalate and ethylene glycol. The obtained hydrolysate is used directly as a feedstock for a terephthalate-degrading *Pseudomonas umsongensis* GO16, also evolved to efficiently metabolize ethylene glycol, to produce PHA. The strain is further modified to secrete hydroxyalkanoyloxy-alkanoates (HAAs), which are used as monomers for the chemo-catalytic synthesis of bio-PU. In short, a novel value-chain for PET upcycling is shown that circumvents the costly purification of PET monomers, adding technological flexibility to the global challenge of end-of-life management of plastics.

1. Introduction

One of the challenges humankind faces is the shift to a sustainable plastic industry. In 2018, 359 million tons of plastics have been produced worldwide and this number is growing at a rate of approximately 3% per *annum* (PlasticsEurope, 2018). Of all the plastic ever produced, only 9% was recycled and 12% was incinerated. The remaining majority is either in use or was landfilled, with a high likelihood to be released into the environment (Geyer et al., 2017). Indeed, in 2010 an estimated 5–13 million tons of plastic ultimately ended up in the ocean (Jambeck et al., 2015). While plastic, due to its lightweight and sturdiness, has many environmentally beneficial applications, the environmental damage caused by plastic must be arrested by addressing the end-of-life challenge.

Abbreviations: EG, ethylene glycol; TA, terephthalic acid terephthalate; PET, polyethylene terephthalate; PHA, polyhydroxyalkanoate; HAA, hydroxyalkanoyloxy-alkanoate; MHET, mono-(2-hydroxyethyl)TA; LCC, leaf-branch compost cutinase.

* Corresponding author.
** Corresponding author. UCD Earth Institute and School of Biomolecular and Biomedical Science, BEACON - Bioeconomy Research Centre, University College Dublin, Belfield, Dublin 4, Ireland
E-mail addresses: kevin.oconnor@ucd.ie (K. O'Connor), lars.blank@rwth-aachen.de (L.M. Blank).
[1] These authors contributed equally to the work.
[2] Present address for Ren Wei: Junior Research Group Plastic Biodegradation, Institute of Biochemistry, University of Greifswald, Felix-Hausdorff-Str. 8, 17489 Greifswald, Germany.

https://doi.org/10.1016/j.ymben.2021.03.011
Received 14 September 2020; Received in revised form 24 February 2021; Accepted 13 March 2021
Available online 16 April 2021

State-of-the-art plastic recycling is either *via* mechanical or chemical methods, or a combination thereof (Ragaert et al., 2017). While mechanical and solvent-based chemical methods focus on a polymer-to-polymer strategy, specific cleanness and properties of plastics waste feedstocks will determine the success of recycling (Ügdüler et al., 2020; Walker et al., 2020). An ideal plastic for recycling is polyethylene terephthalate (PET). The main PET product, beverage bottles, can be specifically collected, avoiding mixed material challenges. In addition, with its thermoplastic properties such as high melting temperature and the possibility to process it without the use of additives, PET fulfils many technical recycling criteria. While in some European countries, PET is collected at quotas above 95% (from single-use beverage bottles), only approximately 30% of it is recycled, even under these ideal conditions (Wierckx et al., 2015). Reasons are manifold including cost, consumer acceptance, and safety regulations surrounding recycled material, to name a few. An alternative way to increase plastic recycling is to add additional value to the plastic waste, not aiming for the same material or consumer good (e.g., bottle-to-bottle recycling), but rather upcycling to chemicals and materials of higher value. This concept has already been demonstrated using chemical methods such as glycolization (Rorrer et al., 2019), alcoholysis (Zhou et al., 2019), glycolysis (Al-Sabagh et al., 2016a; Wang et al., 2012), and organocatalysis (Jehanno et al., 2018).

This upcycling can also potentially be achieved by using carbon-rich plastic waste streams as a substrate for biotechnological processes (Wierckx et al., 2015). Here, PET is depolymerized into its monomers terephthalic acid (TA) and ethylene glycol (EG) and this "plastic hydrolysate" is used as carbon and energy feedstock for microbes that produce valuable molecules and materials. In principle, as we see it (Wierckx et al., 2015, 2018), plastic waste biotechnology mirrors the well-known utilization of lignocellulosic hydrolysate: i) Hydrolysis of the polymeric substrate, ii) metabolism of the resulting hydrolysates by microorganisms, and iii) production of value-added chemicals and polymers by these organisms. However, unlike plant biomass, plastics are often chemically less complex consisting of only a few well-defined monomers, making them potentially much easier substrates for biotechnological utilization. PET, for instance, is a highly pure polymer compared to biomass, composed of almost 100% EG and TA (Wei et al., 2019a; de Ilarduya and Munoz-Guerra, 2014). In the context of plastic waste biotechnology, enzymatic PET depolymerization would be ideal. It features high carbon efficiency and clean and safe reaction conditions, and also yields highly biocompatible hydrolysates. However, the microbial degradation of lignocellulose, which is biotechnologically challenging by itself (Olson et al., 2012), has the benefit of hundreds of millions of years of evolutionary optimization. In contrast, plastics have only entered the biosphere in the last century. The need for optimization of biotechnological catalysts thus becomes obvious. Enzymes, microbes, and processes are required that are capable of degrading synthetic polymers previously considered as non-biodegradable with high rates.

In 2016 the bacterium *Ideonella sakaiensis* was reported to degrade amorphous PET when cultured in the presence of yeast extract as an additional carbon source (Yoshida et al., 2016). The molecular basis of the ester-bond hydrolyzing PETase and mono-(2-hydroxyethyl)TA (MHET)ase enzymes of this strain was reported in several publications (e.g., (Palm et al., 2019; Austin et al., 2018)). The biodegradation of these recalcitrant plastics is an exciting discovery that give hope for the natural bioremediation of sites contaminated with plastic waste in the environment, although plastic degradation in the ocean seems to be slow at best and the anthropogenic dissemination of new plastic pollution likely far exceeds its decay (Jacquin et al., 2019). However, the majority of commercially used PET is a semi-crystalline polymer with a significant amorphous content, which is particularly amenable to enzymatic depolymerization at its glass transition temperature of about 70 °C (Wei and Zimmermann, 2017a). Therefore, compared to the mesophilic *I. sakaiensis* enzymes, counterparts from thermophilic microorganisms stable at >70 °C emerged as more promising biocatalysts for the rapid degradation of PET plastic waste (Wei et al., 2019a, 2019b). Recently, Tournier et al. demonstrated a rapid depolymerization (>90%) of amorphized post-consumer PET waste using an engineered PET hydrolase at 72 °C within 10 h at an industrial relevant scale, yielding highly pure TA that was subsequently used to synthesize virgin PET with properties as those derived from petroleum-based TA (Tournier et al., 2020).

Here, we present the biocatalytic upcycling of PET into two types of biopolymers using a multidisciplinary approach (Fig. 1). PET was hydrolyzed enzymatically in a dedicated reactor into its monomers EG and TA. The monomers were converted by a modified *Pseudomonas umsongensis* GO16 into the native intracellular polymer polyhydroxyalkanoate (PHA) and into the engineered extracellular building block hydroxyalkanoyloxy-alkanoate (HAA). After HAA purification, this platform molecule (Meyers et al., 2019) was chemically co-polymerized to form a novel partly bio-based poly(amide urethane) (bio-PU). In short, we present novel sequential bio-upcycling routes for PET waste, adding technological flexibility to the global challenge of sustainable end-of-life management of plastics.

2. Materials and methods

2.1. Chemicals

Suprasec 2385 (uretonimine-modified 4,4′-diphenylmethylene diisocyanate (4,4′-MDI)) was supplied by Huntsman. 1,4-butanediol (1,4-BDO) (99%), N,N-dimethylformamide (DMF), ethyl acetate, pyridine, p-toluenesulfonic acid (p-TSA), oxalyl chloride (98%), deuterated chloroform ($CDCl_3$) and deuterated dimethyl sulfoxide (DMSO-d_6) were purchased from Sigma-Aldrich. All solvents used for the analytical methods were of analytical grade.

2.2. Bacterial strains and plasmids

Strain *P. umsongensis* GO16 (accession number NCIMB 41538, NCIMB Aberdeen, Scotland, UK) was used for PHA and HAA synthesis. *Escherichia coli* BL21 (DE3) was used to produce the recombinant polyester hydrolase LC-cutinase (Sulaiman et al., 2012). *P. umsongensis* GO16

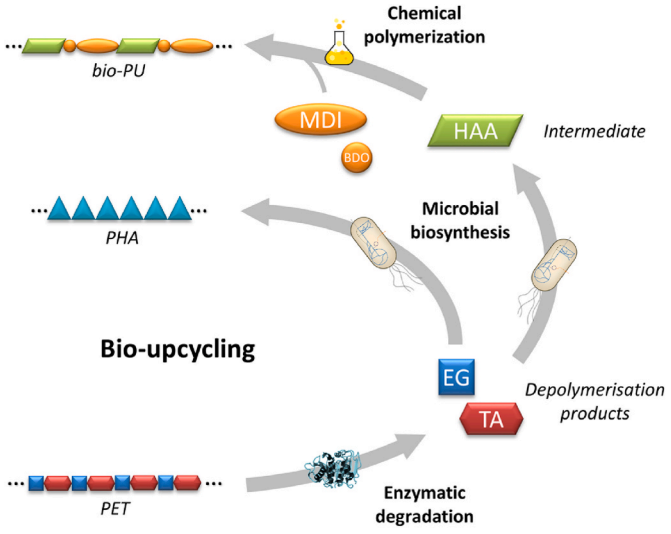

Fig. 1. Two alternative bio-upcycling routes for PET waste to biopolymers. PET hydrolysis is catalyzed by a thermostable polyester hydrolase. The resulting monomers EG and TA (blue and red, respectively) are fed to an engineered *P. putida*, which synthesizes either extracellular HAA (green), or the intracellular biopolymer PHA (cyan). While PHA is already a polymer, HAA is co-polymerized with a diisocyanate and butanediol (orange) to yield a novel bio-based poly(amide urethane) (bio-PU).

KS3 was transformed with pSB01, the plasmid mediating HAA synthesis constructed previously (Tiso et al., 2017).

2.3. LC-cutinase production

The recombinant enzyme production was carried out in *E. coli* BL21 (DE3) harboring pET-20b(+) containing the synthetic gene (Schmidt et al., 2016) (ENA: LN879395) encoding an leaf-branch compost cutinase (LCC), which was originally identified from a plant compost metagenome. A 42-L fermenter (Infors AG, Bottmingen, Switzerland) with a working volume of 25 L was used to produce recombinant LCC as described previously for a homologous polyester hydrolase (Roth et al., 2014).

Briefly, the recombinant *E. coli* culture was grown at 37 °C to an optical density at 600 nm (OD_{600}) of 1.5. The recombinant protein production was induced at a final IPTG concentration of 0.5 mM at 18 °C for 14 h. Bacterial cells were harvested by centrifugation at 11,285×*g* and 4 °C for 25 min. Cell pellets were resuspended in 50 mM sodium phosphate buffer (pH 8) containing 300 mM NaCl and disrupted by ultra-sonication. Following the removal of cell debris by centrifugation, the resulting supernatant containing soluble LCC was subjected to purification by immobilized metal ion chromatography (IMAC) using Ni-NTA Superflow (Qiagen, Hilden, Germany). Protein elution using 250 mM imidazole was then dialyzed against 100 mM potassium phosphate buffer (pH 8) prior to the application in the enzymatic PET hydrolysis. Protein content was determined using the Bradford method. The esterolytic activity was determined using *para*-nitrophenyl butyrate (*p*-NPB) as a substrate as described elsewhere (Oeser et al., 2010). One unit esterolytic activity was defined as the amount of enzyme required to hydrolyze 1 μmol of *p*-NPB per min.

2.4. Enzymatic hydrolysis of PET

The enzymatic hydrolysis of PET was carried out in a 1 L temperature controlled stirred tank reactor (STR, Duran Group GmbH, Wertheim/Main, Germany). Approximately 15.7 g of amorphous PET film (surface of 1,000 cm^2) (product number ES301445, Goodfellow Cambridge Ltd., Huntingdon, UK) were cut into pieces of about 2 × 2 cm^2, and then washed with 0.1% SDS, ethanol, and ultra-pure water, followed by drying at 50 °C for 24 h. Cleaned PET film pieces were placed in the STR containing 400 mL of 27 μg/mL IMAC purified LCC dissolved in 1 M potassium phosphate buffer (pH 8). The hydrolytic reaction was conducted at a constant temperature of 70 °C and an agitation speed of 100 rpm. Samples of 4 mL were removed from the reaction supernatant at time points 0, 2, 4, 6, 8, 24, 48, 72, 96, 120 h for offline analytics. The amounts of terephthalic acid (TA) and ethylene glycol (EG), and their mono-ester (MHET) and di-ester (BHET) released from the PET bulk polymer as well as the residual esterolytic activity against *p*-NPB and the pH in the reaction supernatant were determined. The resulting soluble reaction supernatant obtained by filtration using a paper filter was transferred to the microbial conversion.

2.5. Adaptive laboratory evolution

As *P. umsongensis* GO16 was not able to metabolize EG, adaptive laboratory evolution was carried out with the constant selective pressure of EG as the sole carbon source. 15 mM of EG were used and the cells were passaged approximately once a day when the stationary phase was reached. This experiment was carried out in shake flasks as repetitive batch culture in duplicates and continued for almost 50 days.

2.6. Impact on growth of the hydrolysis solution

To investigate whether growth inhibiting compounds are contained in the product solution of the enzymatic hydrolysis, the two wild-type strains *P. putida* KT2440 and *P. umsongensis* GO16 were cultivated in 24-deep well plates in the Growth Profiler 960 (Enzyscreen B.V., Heemstede, The Netherlands) with 1 mL filling volume at 300 rpm and a throw of 50 mm.

Adapted mineral salt medium (Hartmans et al., 1989), here called Delft medium, with the standard phosphate buffer capacity increased 3-fold (11.64 g/L K_2HPO_4, 4.89 g/L, NaH_2PO_4, 2 g/L $(NH_4)_2SO_4$, 10 mg/L EDTA, 100 mg/L $MgCl_2 \times 6\ H_2O$, 2 mg/L $ZnSO_4 \times 7$ H2O, 1 mg/L $CaCl_2 \times 2\ H_2O$, 5 mg/L $FeSO_4 \times 7\ H_2O$, 0.2 mg/L $Na_2MoO_4 \times 2\ H_2O$, 0.2 mg/L $CuSO_4 \times 5\ H_2O$, 0.4 mg/L $CoCl_2 \times 6\ H_2O$, 1 mg/L $MnCl_2 \times 2\ H_2O$). The water used to prepare the medium was supplemented with increasing amounts of the hydrolysate (5%, 10%, and 20% v/v).

2.7. PHA production

To demonstrate the conversion of hydrolyzed PET into biodegradable polymer PHA, the evolved strain KS3 was grown in a 5 L bioreactor. The cultures were prepared as follows.

P. umsongensis GO16 KS3 was inoculated from a glycerol stock onto mineral salts medium (MSM) solidified with 1.5% agar supplemented with 4.4 g/L (20 mM) disodium terephthalate (TA; Sigma). MSM contained 9 g/L $Na_2HPO_4 \cdot 12H_2O$, 1.5 g/L KH_2PO_4, and 1 g/L (MSM_{full}) or 0.25 g/L (MSM_{lim}) NH_4Cl. Prior to inoculation MSM was supplemented with $MgSO_4$ (200 mg/mL) and trace elements (per liter: 4 g $ZnSO_4 \cdot 7H_2O$; 1 g $MnCl \cdot 4H_2O$; 0.2 g $Na_2B_4O_7 \cdot 10H_2O$; 0.3 g $NiCl_2 \cdot 6H_2O$; 1 g $Na_2MoO_4 \cdot 2H_2O$; 1 g $CuCl \cdot 2H_2O$; 7.6 g $FeSO_4 \cdot 7H_2O$). A single colony was inoculated into 3 mL of MSM_{Full} supplemented with 20 mM TA and incubated for 18 h at 200 rpm and 30 °C. The seed cultures for the bioreactor experiments were prepared in 50 mL MSM_{full} supplemented with a synthetic mixture of 3.32 g/L (20 mM TA) and 1.24 g/L (20 mM) EG, cultivated for 18 h at 200 rpm and 30 °C.

P. umsongensis GO16 KS3 was cultivated in a 5 L stirred tank bioreactor (Sartorius UniVessel Glass 5 l) containing 3 L of MSM_{lim} broth. The bioreactor was inoculated with 150 mL of seed culture. Each cultivation was run for 28 h at constant temperature of 30 °C. Air was sparged at a rate of 3 L/min and a Rushton impeller was utilized for each experiment with a minimum stirring rate of 500 rpm. All parameters were automatically controlled to maintain a minimum dissolved oxygen (DO) level above 20% and a pH of 7.0 ± 0.1 *via* the addition of 5 M NaOH and 15% (vol/vol) H_2SO_4 to impose inorganic nutrient limitation and therefore stimulate PHA accumulation. The hydrolyzed PET was supplied at the amount to yield 40 mM of each TA and EG. Three 2 mL samples were taken at regular intervals for the analysis of TA, EG and nitrogen concentrations, biomass, and PHA accumulation for each time point. The samples were centrifuged at 16,000 *g* for 3 min. The supernatant was collected and stored at -20 °C prior to analysis, while the cell pellet was stored at -80 °C and subsequently lyophilized (Labconco FreeZone 12 bulk tray freeze drier, USA) for 24 h and weighed.

2.8. Production of HAA

The medium for HAA synthesis was Delft medium. The monomer solution from PET hydrolysis was diluted 1:20 and autoclaved. This solution was used to prepare the medium instead of water. HAA was produced and purified as shown previously (Tiso et al., 2017).

2.9. Direct HAA polymerization to poly(amide urethane)

The direct HAA polymerization to poly(amide urethane) was performed with an isocyanate to hydroxyl and acid molar ratio ([NCO]/([OH] + [COOH])) equal to 2 and without catalyst addition. In a round bottom flask of 50 mL, the appropriate amount of HAA (505 mg) and modified 4,4′-MDI (787 mg) were introduced under nitrogen flux. The reaction mixture was heated up to 90 °C and magnetically stirred for 4 h under nitrogen flux. After 5 min of reaction, 1 mL of N,N-dimethylformamide (DMF) solvent was added to keep an efficient stirring. This solvent addition was repeated after 60 min of reaction. After 4

h of reaction, a determined amount of 1,4-butanediol (1,4-BDO) (20 mg) was added and the polymerization was allowed to proceed for an additional 1 h. The reaction product was then dried under vacuum at 80 °C for 16 h to remove DMF. The final product was recovered as a yellowish solid.

2.10. Analytics

2.10.1. PHA extraction and content determination

The polymer content was assayed by subjecting the lyophilized cells to acidic methanolysis as previously described (Lageveen et al., 1988). The PHA monomers' methylesters were assayed by GC using a Hewlett-Packard 6890 N chromatograph equipped with a HP-Innowax capillary column (30 m × 0.25 mm, 0.50-μm film thickness; Agilent Technologies) and a flame ionization detector (FID), using the temperature program previously described (Lageveen et al., 1988). Total PHA content was determined as a percentage of cell dry weight (CDW).

2.10.2. Nitrogen quantification

The concentration of nitrogen in the media was monitored by taking 1 mL samples from the cultures at various time points and centrifuging them for 3 min at 16900×*g* (benchtop 5430R centrifuge; Eppendorf, Germany). The supernatant was retained and the nitrogen concentration was determined using the method of Scheiner et al. (Scheiner, 1976). Briefly, the supernatant was diluted to 10^{-3} in deionized water and placed in a 1 cm path length, 1.6 mL volume cuvette (Sarstedt, Germany). 400 μl of phenol solution (per 100 mL of deionized water: 1.3 g Na_3PO_4; 3 g $Na_3C_3H_5O_7$; 0.3 g sodium EDTA; 6 g phenol; 0.02 g sodium nitroprusside) was added to the cuvette and mixed well. This was promptly followed by the addition of 600 μl of alkaline solution (per 100 mL of final volume: 40 mL 1 M NaOH; 2.5 mL hypochlorite solution; 57.5 mL deionized water). The mixture was incubated at room temperature in the dark for 45 min. The formation of indophenol-blue was measured at 635 nm using the Unicam Helios δ UV/VIS spectrophotometer (Thomas Scientific, USA).

2.10.3. HAA quantification

HAA was quantified using high-performance liquid-chromatography coupled with a charged aerosol detector using a method established earlier (Tiso et al., 2017).

2.10.4. EG quantification

For the PHA production experiments, EG depletion was monitored using on an Aminex HPX-87H ion exclusion column (300 mm × 7.8 mm, particle size 9 μm; Bio-rad). The column was maintained at 40 °C and samples were isocratically eluted using 0.014 N H_2SO_4 at a flow rate of 0.55 mL/min and read on a refractive index detector (RID). The EG retention time under the above conditions was 23 min.

For the HAA synthesis experiments, an ion exchange chromatography was applied for EG quantification. The used System Gold was composed of a pump LC-126, an autosampler LC-508, a Jetstream 2 Plus column oven (Knauer, Berlin, Germany), and a refractive index detector Smartline RI Detector 2300 (Knauer, GmbH, Berlin, Germany). The applied column was the Metab-AAC (ISERA GmbH, Düren, Germany) with a length of 30 cm and a diameter of 7.8 mm. The running buffer was 5 mM sulfuric acid, which was pumped isocratically with a flow rate of 0.8 mL/min at a temperature of 80 °C. 20 μL of the sample were injected.

2.10.5. TA quantification

For the PHA production experiments, the supernatant collected during growth was diluted 20-fold and filtered (500 μl) using Mini-UniPrep syringeless filter devices (GE Healthcare Life Science, Ireland). TA concentration was analyzed according to the protocol previously outlined by Kenny et al. (2008).

For the HAA synthesis experiments, the amounts of the UV-absorbing degradation products in the STR samples were measured by reversed-phase HPLC as described before (Barth et al., 2015). A C18 column (Eurospher 100-5, 150 mm × 4.6 mm with pre-column, Knauer GmbH, Berlin, Germany) and a mobile phase consisting of 20% acetonitrile, 20% 10 mM sulfuric acid and 60% ultra-pure water was used. The hydrolysis supernatant samples were diluted using the mobile phase, acidified with concentrated HCl (37%) and then centrifuged to remove any precipitation. The detection of TA and associated low-molecular-weight (LMW) esters was performed at a wavelength of 241 nm.

2.10.6. HAA-based poly(amide urethane) characterization

^{1}H- and ^{13}C-NMR spectra were obtained with a Bruker 400 MHz spectrophotometer. $CDCl_3$ and DMSO-d_6 were used as deuterated solvent to prepare solutions with concentrations of 8–10 and 30–50 mg/mL for ^{1}H-NMR and ^{13}C-NMR, respectively. The number of scans was set to 128 and 1024 for ^{1}H- and ^{13}C-NMR, respectively. Spectra were calibrated using the $CDCl_3$ peak ($\delta_H = 7.26$ ppm, $\delta_C = 77.16$ ppm) or the DMSO-d_6 peak ($\delta_H = 2.50$ ppm, $\delta_C = 39.52$ ppm).

Fourier transformed infrared spectroscopy (FTIR) was performed with a Nicolet 380 spectrometer (Thermo Electron Corporation) used in reflection mode and equipped with an ATR diamond module (FTIR-ATR). The FTIR-ATR spectra were collected at a resolution of 4 cm^{-1} and with 32 scans per run.

Differential scanning calorimetry (DSC) was performed using a TA Instrument Q200. Samples of 2–3 mg in sealed aluminum pans were analyzed under nitrogen flow (50 mL/min). A three-step procedure with a 10 °C/min ramp was applied as follow: (1) heating up from room temperature to 200 °C and holding for 3 min to erase the thermal history, (2) cooling down to -60 °C and holding for 3 min, (3) heating up (second heating) from -60 °C to 200 °C.

Thermal stability was studied by thermogravimetric analyses (TGA). Measurements were conducted under air atmosphere (flow rate of 25 mL/min) using a Hi-Res TGA Q5000 apparatus from TA Instruments. Samples (1–3 mg) were heated from room temperature up to 800 °C at a rate of 10 °C/min.

2.11. Flux balance analysis

FBA has been carried out as described previously (Bator et al., 2020). Briefly, the genome-scale metabolic model of *P. putida* KT2440, *i*JN1411, was used (Nogales et al., 2017, 2019) and extended by the biosynthesis routes for HAA production and the metabolization routes for EG and TA. All simulations were carried out in MATLAB (version R2017b, The Mathworks, Inc., Natick, MA, USA) using the COBRA toolbox (Schellenberger et al., 2011; Heirendt et al., 2019), with the linear programming solver of Gurobi (www.gurobi.com).

The added reactions are: (i) HAA synthesis based on two R-3-hydroxydecanoyl-ACP from fatty acid *de novo* synthesis, (ii) EG metabolization using the pathway proposed earlier (Li et al., 2019) with glyoxylate being the product, which is subsequently metabolized *via* existing reactions in the model, and (iii) TA degradation, which includes the *tph* operon and a further step for the formation of protocatechuate as described previously for *P. umsongensis* GO16 (Narancic et al., 2021).

(i) HAA from R-3-hydroxydecanoyl-ACP

$$2\ C_{10}H_{19}O_2ACP + H_2O \Leftrightarrow C_{20}H_{38}O_5 + 2\ \ ACP$$

(ii) Ethylene glycol to glyoxylate

$$C_2H_6O_2 + PQQ + NAD^+ + 2\ \ Cyt^{Ox} + 3\ \ H_2O \Leftrightarrow C_2HO_3 + PQQH_2 + NADH + 2\ \ Cyt^{Red} + 3\ \ H^+$$

(iii) Terephthalic acid to protocatechuate

$$C_8H_6O_4 + O_2 \Leftrightarrow C_7H_6O_4 + CO_2$$

3. Results

3.1. Enzymatic PET degradation

The here presented interdisciplinary approach for the upcycling of PET is initiated by enzymatic cleavage of the polymer. Microbial polyester hydrolases capable of efficiently degrading amorphous or low-crystallinity PET samples (Wei and Zimmermann, 2017b) at elevated temperatures close to the glass-transition temperature have been found in fungi (Ronkvist et al., 2009), thermophilic actinomycetes (e.g., (Wei et al., 2019a; Müller et al., 2005; Then et al., 2016; Wei et al., 2014a)), and in plant compost (Sulaiman et al., 2012). The here used leaf-branch compost cutinase (LCC) is a polyester hydrolase, of which the encoding gene was originally isolated from a plant compost metagenome (Sulaiman et al., 2012). This enzyme appeared to be the most active wild-type thermophilic PET hydrolase published so far (Wei et al., 2019b). By applying an enzyme concentration of the wild-type LCC in the range of 1–2 mg_{enzyme}/g_{PET}, a depolymerization degree of >50% has been reported after 24 h at 70–72 °C, either with amorphous PET films in reaction tubes (Falkenstein et al., 2020) or with amorphized post-consumer PET waste in a bioreactor (Tournier et al., 2020). The enzyme was produced in *E. coli* and purified as described previously (Schmidt et al., 2017).

A single scaled-up PET hydrolysis experiment was carried out to generate the material for the subsequent steps. Fig. 2 shows the time courses of the formation of the degradation products released from amorphous PET films during LCC-catalyzed hydrolysis in a stirred tank reactor (STR), as well as of the pH values determined in the reaction supernatant. The concentration of TA and EG showed a steep near-linear increase at a maximum rate of 4.1 mM/h and 2.1 mM/h, respectively, within the first 24 h of the hydrolytic reaction and weakened to a markedly lower rate (close to 0 mM/h for both TA and EG) until 120 h. By contrast, the amount of MHET increased gradually in the early stage of the reaction and peaked at 24 h, followed by a slow decline until 120 h. Concomitantly, the release curve of bis-(2-hydroxyethyl)TA (BHET) showed a similar shape with the maximum value determined after 8 h of less than 3 mM. In previous studies, MHET and BHET were found to be inhibitors for polyester hydrolases including LCC (e.g., (Barth et al., 2015; Barth et al., 2016)). Therefore, LCC was assumed to preferably catalyze the depolymerization of PET during the first 24 h, followed by a detectable cleavage of MHET and BHET afterwards. Based on the molecular weights of these small molecules, the depolymerization degree of PET polymer in percentages could be estimated. The Goodfellow amorphous PET film used in this study has previously been shown to have an initial number-average molecular mass (Mn) of approximately 33,300 g/mol determined by a solution NMR-based method (Wei et al., 2019a). The degree of depolymerization, which is indeed a measure of the decrease in Mn of the PET polymers, has been previously shown to be in a near linear correlation with the determined weight losses (Wei et al., 2019a). Fig. 2 indicates that over 47% depolymerization of the amorphous PET films (15.7 g) was achieved within the first 24 h, which remained almost unchanged until 120 h. This was assumed to be the result of gradually denatured biocatalysts under thermophilic condition (70 °C), as suggested by Tournier et al. (2020) and based on the esterolytic activities determined in the reaction supernatant in this study (data not shown). In addition, the continuous pH decrease in the first 24 h resulting from the rapid release of TA even though a high buffer concentration of 1 M potassium phosphate was used may also contribute to the enzyme inactivation.

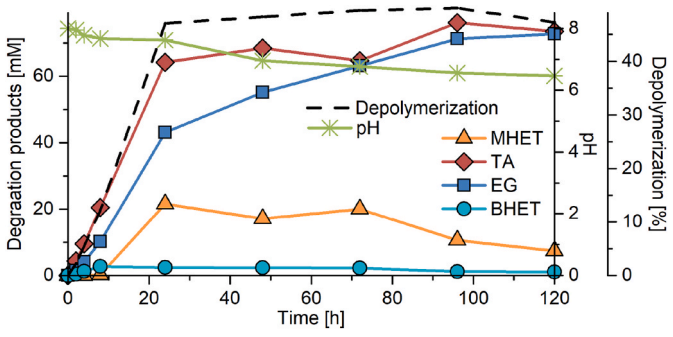

Fig. 2. PET film hydrolysis. Time courses of PET hydrolysis into (soluble) ethylene glycol (EG), terephthalic acid (TA), mono-(2-hydroxyethyl)TA (MHET), and bis-(2-hydroxyethyl)TA (BHET) (primary y-axis) catalyzed by purified wild-type LCC in a stirred tank reactor at 70 °C, as well as of pH value in the reaction supernatant (secondary y-axis). Besides, the estimated degree of depolymerization (dashed line) based on the products release is plotted (tertiary y-axis). Data from a single representative experiment.

In the study of Tournier et al. TA was recovered by acid precipitation and crystallization from the PET hydrolysate. In contrast, we here aim at direct utilization of the post-reaction broth from the enzyme reactor without prior purification, allowing the use of both TA and EG. Our approach thus entails potentially lower cost and a much higher recycling ratio.

3.2. Towards upcycling of enzymatically hydrolyzed PET

Two different pathways were employed for the biosynthesis of molecules for bioplastic production using *Pseudomonas*. Pseudomonads are Gram-negative bacteria with a high potential for degrading synthetic plastics (Wierckx et al., 2015; Wilkes and Aristilde, 2017), due to their versatile arsenal of catabolic enzymes (Tiso et al., 2015). Different *Pseudomonas* strains are known for their metabolism of a wide variety of substrates, including aromatics such as TA (Kenny et al., 2008), and aliphatics such as EG (Franden et al., 2018; Li et al., 2019; Mückschel et al., 2012). Indeed *P. umsongensis* GO16, isolated from a PET bottle processing plant is able to metabolize TA as the sole source of carbon and energy and was previously used to produce the biodegradable polymer PHA from TA emanating from pyrolyzed PET (Kenny et al., 2008). A companion study to this has investigated the metabolic capacity of the strain GO16, identifying the genes responsible for TA and EG metabolism, for the metabolism of many aromatics, and for PHA synthesis (Narancic et al., 2021).

3.2.1. Enzymatic hydrolysis product is non-toxic for Pseudomonas

The question if the PET hydrolysate inhibits growth of the employed bacteria was addressed first. Wild-type strains *P. putida* KT2440 and *P. umsongensis* GO16 were grown in minimal medium supplied with 10 g/L of glucose and increasing amounts of the hydrolysate solution (from 0 to 20%). *P. putida* KT2440 showed no significant differences in growth when exposed to varying concentrations of the PET hydrolysate (Fig. 3). *P. umsongensis* GO16 did not show any growth inhibition either. In contrast it seemed that growth was enhanced with increasing hydrolysate concentrations. These gain in fitness is most likely based on the ability of *P. umsongensis* GO16 to be able to use TA as an additional carbon source. We thus conclude that compounds inhibiting growth of the here used bacteria are not present in the enzymatic PET hydrolysate.

3.2.2. Growth of P. umsongensis GO16 on PET monomers

To enable conversion of both monomers of PET into value added products, the metabolism of EG had to be improved. We observed that *P. umsongensis* GO16 was capable of slow growth on EG with a lag phase of more than 5 days. This growth was improved by adaptive laboratory evolution as also shown previously for *P. putida* KT2440 (Li et al., 2019). During about 45 days 15 sequential batch cultivations were carried out. After evolving for approximately 100 generations, the evolved strain *P. umsongensis* GO16 KS3 was able to grow on EG at a rate of 0.4 1/h while the wild-type strain did only show slow growth (μ = 0.14 1/h)

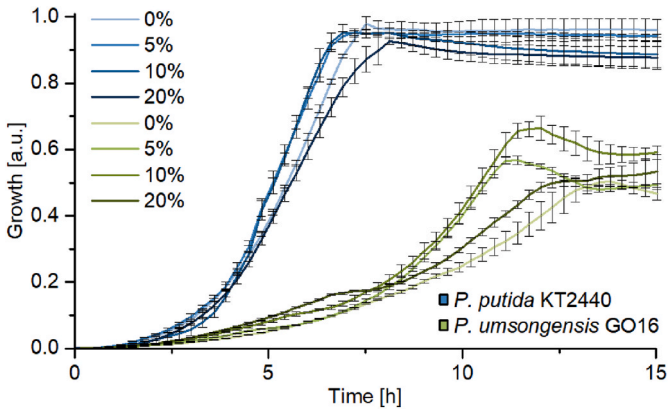

Fig. 3. Impact on growth of the enzymatic PET hydrolysate. Wild-type strains *P. putida* KT2440 (blue) and *P. umsongensis* GO16 (green) were grown on glucose with increasing amounts of the hydrolysis solution (the darker the color, the higher the hydrolysate share). The error bars represent the standard deviation from the mean of three independent biological replicates.

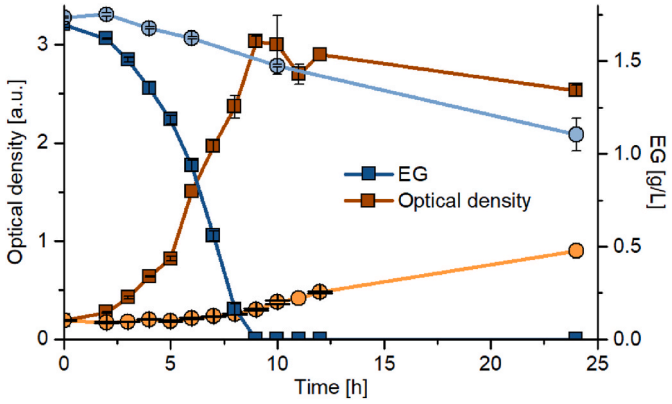

Fig. 4. Laboratory evolution of *P. umsongensis* GO16 for enhanced ethylene glycol (EG) metabolization. *P. umsongensis* GO16 wild type and the evolved *P. umsongensis* GO16 KS3 grown on EG as sole carbon source in shake flasks. The orange colors present growth (OD_{600}; a.u. – absorbance units) while the blue colors show the EG concentrations (brighter colors and circles – wild-type strain; darker colors and squares – evolved strain). The error bars represent the standard deviation from the mean of three independent biological replicates.

(Fig. 4). HPLC analysis revealed that the evolved strain was able to completely deplete 1.7 g/L of EG in around 9 h, while only minor EG consumption was observed for the wild-type strain. As described by Li et al. (2019), EG can be used as carbon source *via* the key enzyme glyoxylate carboligase, forming the C3 metabolite tatronate semialdehyde from two glyoxylates (Fig. 6). This C3 metabolite is in the subsequent enzymatic steps converted to pyruvate. In the presence of an alternative carbon source, EG can be used as energy donor only. Thereby, EG is also oxidized to glyoxylate, but subsequently funneled into the TCA cycle *via* the glyoxylate shunt yielding two CO_2 and redox equivalents.

3.2.3. Synthesis of the biopolymer polyhydroxyalkanoate (PHA)

The monomers obtained by enzymatic PET hydrolysis were firstly used for the conversion into PHA using *P. umsongensis* GO16 KS3. PHAs are a family of bacterial carbon and energy storage polyesters, which represented 1.2% of the global bioplastic market in 2019 (Bioplastics, 2019). With over 150 known PHA monomers, (*R*)-3-hydroxyalkanoic acids, PHAs have highly diverse material properties and therefore a broad range of applications from packaging to medical (Rehm, 2010). The bioconversion of hydrolyzed PET (described above) into PHA was

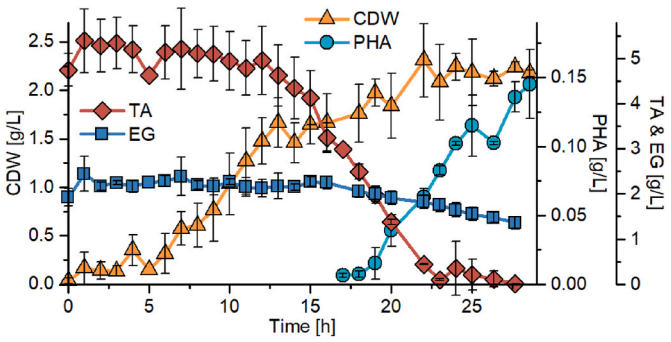

Fig. 5. Growth, PHA accumulation, and substrate depletion by *P. umsongensis* GO16 KS3 in nitrogen limiting conditions with enzymatically hydrolyzed PET as sole carbon and energy source. *P. umsongensis* GO16 KS3 was cultivated in a 5 L bioreactor with 3 L of mineral salts medium (MSM) at 30 °C. The hydrolyzed PET was added to a concentration of approximately 30 mM of each TA and EG. Growth (cell dry weight, CDW), polyhydroxyalkanoate (PHA, %CDW), substrates terephthalic acid (TA) and ethylene glycol (EG). The error bars represent the standard deviation from the mean of three independent biological replicates.

carried out in a 5 L batch reactor. TA was completely consumed by 23 h of cultivation, while EG was consumed at a 3.5-fold lower rate and did not reach complete depletion (Fig. 5). When using a synthetic mixture of TA and EG, the EG depletion rate was much higher (Fig. S1, Supplementary material). The highest biomass achieved was 2.3 g/L after 22 h of incubation, remaining at a similar level for the next 5 h. Nitrogen was completely exhausted after 16 h of cultivation, corresponding to the onset of PHA accumulation. The PHA level kept rising after TA depletion, and reached a maximum of 0.15 g/L representing approximately 7% of cell dry weight (CDW) and indicating that both TA and EG derived from enzymatically hydrolyzed PET were converted into PHA (Fig. 5). A final yield of 0.21 $g_{CDW}/g_{substrate}$ was achieved, including the PHA portion of the biomass. The medium-chain-length PHA produced by *P. umsongensis* GO16 KS3 from hydrolyzed PET consisted of C_{10} (61 mol %), C_{12} (24 mol%), and C_8 (15 mol%). The monomer composition was similar to that observed when TA was used as a sole carbon and energy source (Kenny et al., 2012). The yield of PHA based on total substrate used was 0.014 $g_{PHA}/g_{substrate}$. Further analysis is required to clarify which substrate contributes with what percentage to the PHA accumulation.

The biological conversion of enzymatically hydrolyzed PET into PHA, a high value polymer, presents a proof of concept that can be developed into a bioprocess to upcycle PET. PHAs are of interest due to the fact that they are biodegradable and have many potential applications (Narancic et al., 2020).

3.2.4. Optimal network configuration for HAA synthesis from EG and TA

While many *Pseudomonas* strains are known to natively produce PHAs, pseudomonads have further been engineered to produce a broad palette of other industrially relevant platform chemicals (Tiso et al., 2015; Loeschcke and Thies, 2015; Wynands et al., 2018). Recently, *P. putida* KT2440 was engineered to synthesize HAA, a dimer of 3-hydroxy fatty acids (Figs. 6 and 8). In contrast to many other fatty acid containing molecules, HAAs are secreted into the growth medium (Tiso et al., 2017), resulting in simpler purification that does not rely on cell lysis. HAAs are amphiphilic molecules with surface-active properties and interesting platform chemicals for further bio- or chemo-catalytic conversion (Meyers et al., 2019).

In order to determine theoretical yields and possible metabolic network configurations for HAA synthesis from EG and TA, flux balance analysis (FBA) was conducted. The metabolic network included the conversion of EG and TA to central carbon metabolism (CCM) intermediates and subsequent HAA synthesis (Fig. 6). As objective

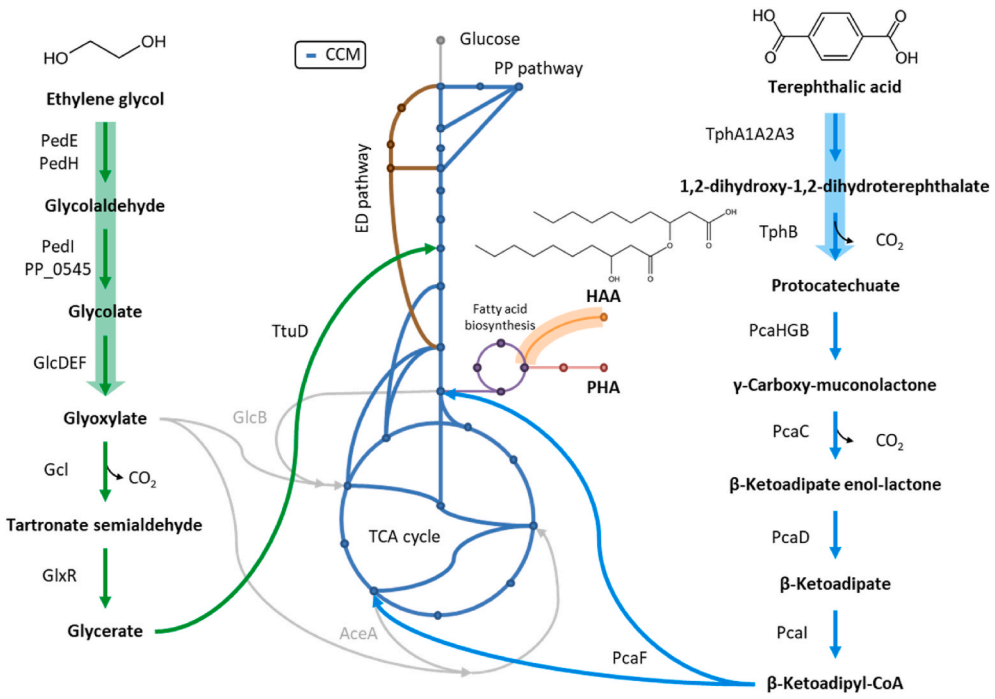

Fig. 6. Metabolic pathways for the metabolization of ethylene glycol (EG) and terephthalic acid (TA). On the left side the enzymatic steps for conversion of EG to the intermediate of the central carbon metabolism (CCM) 2-phospho-glycerate is shown (green). The grey lines represent pathways in which EG serves only as source for redox equivalents and the generation of CO_2. On the right side the conversion of TA to the CCM intermediates succinate and acetyl-CoA is a depicted (light blue). The shaded thick arrows depict reactions that have been added to the metabolic model *i*JN1411.

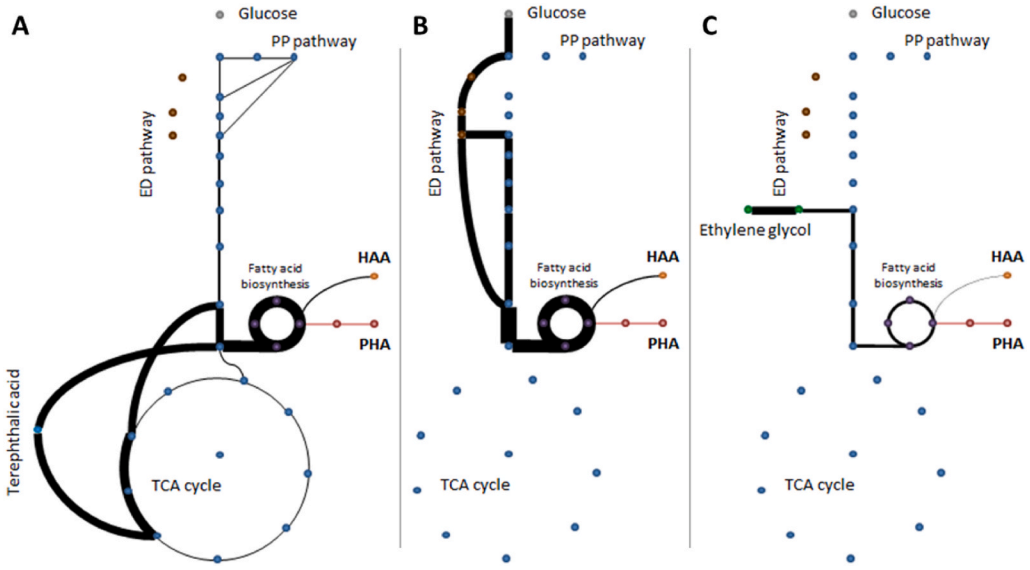

Fig. 7. Optimal flux distributions for HAA synthesis based on different substrates. A) glucose, B) terephthalic acid, and C) ethylene glycol. The thickness of the lines represents the flux rates in absolute values. PP – pentose phosphate, ED – Entner-Doudoroff, TCA – tricarboxylic acid, HAA – hydroxyalkanoyl alkanoic acid.

function product synthesis, here HAA synthesis was chosen. The computed theoretical yields for HAA synthesis are for TA and EG, 0.38 g_{HAA}/g_{TA} and 0.28 g_{HAA}/g_{EG}, respectively. The resulting HAA synthesis rates at a given substrate uptake rate are shown in Table 1. Since the starting material (PET) contains both EG and TA, we further computed flux distribution and yield for a mixture of EG and TA. In this scenario, EG is only used as energy donor, which increases the yield on TA. Due to the high degree of reduction of EG the calculations end up with a composition of 77% TA and 23% EG to not result in an electron surplus.

A further output of FBA was the optimal flux distribution for the scenario of the maximal theoretical yield for both substrates (EG and TA) with glucose as comparison. The results show very distinct flux distribution patterns (Fig. 7). While during glucose metabolization exclusively the Entner-Doudoroff (ED) pathway is active, during degradation of terephthalic acid many pathways are at least partially active. However, also here the major share of resources is fed into fatty acid *de novo* synthesis for the synthesis of the HAAs. Ethylene glycol as carbon source for HAA synthesis is channeled completely towards fatty acid *de novo* synthesis.

The direct conversion of EG might be caused by its high degree of reduction, providing enough redox cofactors for the expensive fatty acid *de novo* synthesis. Direct conversion of TA on the other hand does not provide sufficient redox equivalents and thus pentose phosphate (PP) pathway and tricarboxylic acid (TCA) cycle are needed to pay for HAA synthesis. The metabolization route of glucose provides sufficient redox co-factors making extensive cycling through any of the cyclic pathways unnecessary.

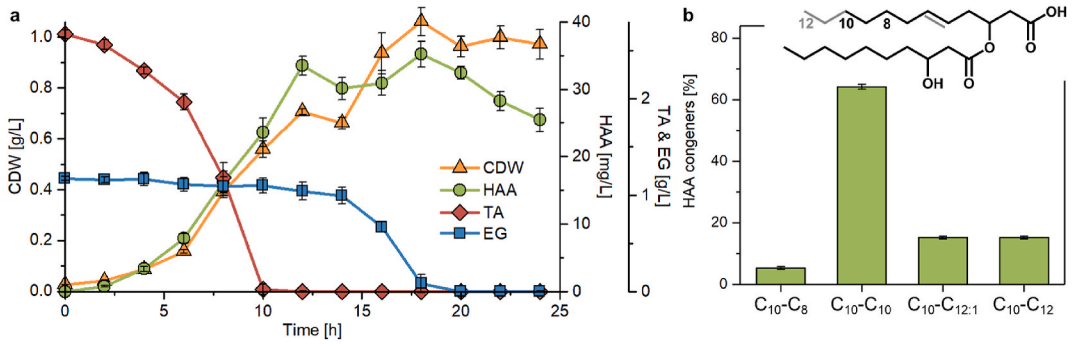

Fig. 8. a) HAA synthesis from hydrolyzed PET. *P. umsongensis* GO16 KS3 pSB01 was cultivated in shake flasks with 50 mL of Delft medium at 30 °C. The PET hydrolysate was added to a concentration of 15–18 mM of each TA and EG. Growth (cell dry weight, CDW), HAA, substrates terephthalic acid (TA) and ethylene glycol (EG) depletion. The error bars represent the deviation from the mean of two biological replicates. b) Molecular diversity of the HAA congeners synthesized from PET monomers. The error bars represent the standard deviation from the mean of two independent cultivations (as indicated in a) at four time points, i.e., eight biological replicates.

Table 1
Theoretical metabolic network performance using terephthalic acid (TA) and ethylene glycol (EG) as carbon and energy source. The key parameters result from FBA.

Substrate	Substrate uptake rate [mol/(g_{CDW} h)]	HAA synthesis rate [mol/(g_{CDW} h)]	Max. theoretical yield [mol/mol]	Max. theoretical yield [Cmol/Cmol]
Glucose	10	2.0	0.20	0.67
Terephthalic acid	10	1.8	0.18	0.46
Ethylene glycol	10	0.5	0.05	0.50
TA:EG (77:23)	TA: 10/EG: 3.1	2.0	0.20	0.50

3.2.5. Biosynthesis of extracellular HAA

In order to demonstrate the production of a non-native value-added molecule from hydrolyzed PET, the evolved *P. umsongensis* GO16 KS3, capable of growth with TA and EG, was transformed with the HAA synthesis plasmid pSB01 (Tiso et al., 2017). The PET hydrolysis solution was diluted to meet the requirements for the microbe and essential nutrients (nitrogen source, trace elements) were added. The resulting concentrations of EG and TA were approximately 15–18 mmol/L each.

With this medium, an HAA concentration of 35 mg/L was achieved (Fig. 8a). During the first 10 h, the TA concentration declined rapidly. EG was only taken up after TA was completely consumed, taking approximately 10 additional hours. However, the engineered strain only synthesized HAA from TA, as HAA reached maximum concentration after 12 h, corresponding to TA depletion. EG apparently was used for growth only, since the cell dry weight increases further while EG is consumed after a short transition phase. The production rate amounted to 5 mg/L/h while the yield was 0.01 g_{HAA}/g_{TA}. The theoretical yield for HAA synthesis from TA is 0.37 g_{HAA}/g_{TA} as determined by flux balance analysis.

The engineered *P. putida* synthesizes a mixture of four HAA congeners as identified by HPLC-CAD (Fig. 8b). The mainly incorporated hydroxy fatty acid detected was hydroxydecanoate. The length of the second monomer varied between eight and twelve carbon atoms, of which the C_{12} can be unsaturated. The HAA structure and composition have been confirmed by ^{1}H NMR analysis (Fig. S2, Supplementary material).

We here show the synthesis of a potential platform molecule for the chemical industry *via* biocatalytic conversion of PET. Being versatile molecules with an amphiphilic structure and multiple functional groups, HAAs have the prospect of being applied in various fields, e.g. as surface-active molecules for cosmetic, food or pharma applications (Tiso et al., 2017). We proceeded to demonstrate their application in the synthesis of a novel partly biobased polymer exploiting the two hydroxy groups in a polymerization reaction.

3.3. Polymerization of HAA

The final stage of the process is the chemical polymerization of the biotechnologically produced HAA to produce a poly(amide urethane) (bio-PU). Such polymers are more complex compared to PET and have different properties and a higher added value. Compared to conventional PU (poly(ether urethane) or poly(ester urethane)) new macromolecular architectures and thus new thermal and/or mechanical properties can be expected (Takeichi et al., 2002; Qin et al., 2019). Since an isocyanate moiety can react with both an hydroxyl and a carboxylic acid group, and HAA is an hydroxy acid, its direct polymerization with 4,4′-methylene diphenyl diisocyanate (MDI) and butanediol (BDO) was performed and led to the formation of a poly(amide urethane). This polymer is still partly based on petrochemical materials. While bio-BDO is available (Burgard et al., 2016), bio-anilin patents (Jaeger et al., 2015) suggest that bio-MDI will be available in the future (Covestro, 2019), to render the synthesized PU completely bio-based. The length of the HAA side chain can be varied depending on the RhlA used for synthesis (Germer et al., 2020), thereby influencing plastic properties.

3.3.1. Direct polymerization to poly(amide urethane)

The polymerization of HAA was based on the mixture of HAA congeners as described previously (Fig. 8b). Direct polymerization with MDI has been carried out by a two-step polymerization involving the synthesis of a prepolymer followed by a chain extension reaction with BDO (Fig. 9).

FTIR and NMR analyses (Fig. 10) indicated simultaneous amide and urethane bond formation, while the reactivity of 4,4′-MDI with the secondary alcohol appeared to be slightly higher than with the carboxylic acid. These analyses confirmed the synthesis of a novel poly (amide urethane).

Differential scanning calorimetry (DSC) analysis of the bio-PU evidenced the amorphous character of the polymer and revealed a glass-transition temperature of 50 °C. This value is consistent with the glass-transition temperature usually reported for polyurethanes obtained from MDI and BDO as main diol, which may vary from 60 to 110 °C (Chen et al., 1997). The slightly lower value obtained here can be explained by the HAA displaying two pendant groups once polymerized with MDI (Fig. 9). These aliphatic pendant groups may increase the chain mobility and can thus be used to tune down the glass-transition temperature in comparison with polyurethane only made from BDO as diol.

The thermal stability of this HAA-based polyurethane was

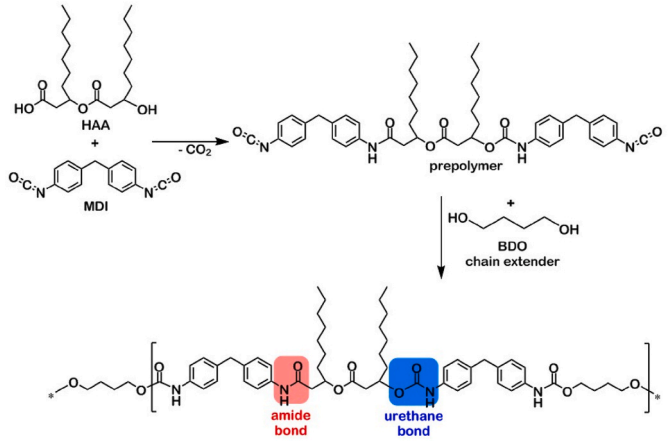

Fig. 9. Novel bio-PU synthesis. Polymerization reaction between the hydroxy fatty acid ester HAA, and MDI diisocyanate. The resulting prepolymer is submitted to chain extension with BDO to form a partly bio-based poly(amide urethane) (bio-PU).

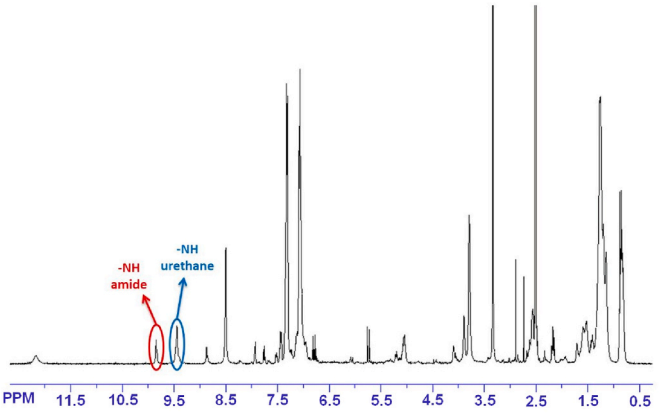

Fig. 10. Confirmation of bio-PU synthesis. ^{1}H NMR spectrum of the final polymer showing the presence of NH signals of both amide (circled in red) and urethane (circled in blue) bonds.

determined by thermogravimetric analysis (TGA). The polymer started to degrade and to lose volatile products at 160 °C and then showed a multi-step degradation profile with the main mass loss occurring between 250 and 350 °C. This behavior is consistent with the thermal stability usually observed for such polymer systems (Rosu et al., 2010; Lee et al., 1994). The rather low onset degradation temperature could be explained by the presence of the ester bond in the HAA, which makes it more sensitive to thermal degradation (the temperature of the maximum degradation rate of HAA is around 215 °C).

4. Discussion

We present the bio-upcycling of plastic waste previously considered non-biodegradable, by cascading the enzymatic depolymerization of PET with the microbial conversion into valuable polymers. This process affords a simple route from commercial PET to biodegradable bioplastic and to HAAs with great biotechnological potential. By using a whole-cell biocatalyst, the hydrolyzed PET can be directly employed as a feedstock, avoiding the need for monomer purification following enzymatic hydrolysis. Renewable plastics including PHA have already been proposed to effectuate a shift of the packaging industry, which consumes over 38% of the plastics produced (Rabnawaz et al., 2017). The results exemplify the previously proposed value-chain for the utilization of plastic waste as additional carbon source in biotechnology to produce a wide range of valuable products (Wierckx et al., 2015, 2018). We see great potential in this new approach to recycling, and thus consider this study a starting point for new research in enzyme technology, strain engineering, and polymer chemistry, akin to the mega-trends in lignocellulosic biotechnology that we have seen in the last decades (Shahzadi et al., 2014; Chundawat et al., 2011).

Lignocellulosic biotechnology has already found solutions to the challenges we are about to face in plastic waste biotechnology. Parameters like high solid loads and enzyme amounts have to be optimized using heuristic approaches and trial-and-error methodologies. As recently demonstrated by Tournier et al., the use of engineered LCC variants may increase the overall degradation performance of amorphized PET waste by up to 80%, causing a >90% depolymerization performance within 10 h (Tournier et al., 2020). This could be even further enhanced, i.e. by combination with chemical hydrolysis methods such as glycolysis (Al-Sabagh et al., 2016b). The use of enzyme cocktails will also enable feedstock flexibility, especially when combined with microbes engineered to accept other plastic-derived substrates. For example, the PET-like polymer polyethylene furanoate (PEF) is also degraded by a PET hydrolase (Austin et al., 2018), and *P. putida* can be engineered to degrade the resulting 2,5-furandicarboxylic acid (Koopman et al., 2010; Guarnieri et al., 2017). It is worth noting that logistics is a major hurdle in lignocellulosic biotech since often completely new infrastructure has to be built (*i.e.*, from forest to factory). In contrast, many countries already have highly efficient plastic waste collection systems, which can find a new valorization through the herein proposed bio-upcycling route.

To achieve the latter will require significant research and technology development. Learning again from lignocellulosic biotech, enzyme discovery and engineering is key for resource- and cost-efficient hydrolysis of the polymers. For PET, the abundance of polyester hydrolases in the environment was investigated in detail. The results suggest that this enzyme activity is rather rare, but more frequent in crude oil rich environments (Wei and Zimmermann, 2017b; Danso et al., 2018; Salvador et al., 2019). Currently further metagenome and mechanistic studies of this important enzyme class are carried out by the scientific community, most likely discovering protein family members with superb activities or at least interesting amino acid variations. The latter can be exploited in protein engineering efforts, already published for the PETase of *I. sakaiensis* (Ma et al., 2018) and thermophilic proteins with the same enzyme specificity (Austin et al., 2018; Wei and Zimmermann, 2017a; Wei et al., 2014b), e.g. with the wild-type LCC by Tournier et al., who indicated that their most promising variant has a considerably higher productivity in terms of TA conversion than the enzymatic degradation of starch and cotton. Tournier et al. reported time courses of depolymerization in a very similar pattern by using the same wild-type LCC to degrade amorphized PET waste in a bioreactor at up to 72 °C, yielding a maximum of 53.9% depolymerization after 24 h reaction. In comparison with our study using 0.69 mg_{enzyme}/g_{PET}, a higher enzyme amount of 1 mg_{enzyme}/g_{PET} was used. Besides, a pH-stat used in their study may help to maintain a more favorable condition for the enzymatic reaction as well as to save buffer agents (0.1 M potassium phosphate buffer used in their study).

Another challenge might be the public perception of novel plastic upcycling technologies, which might be perceived as potentially dangerous. A recent commentary aims at debunking common myths about plastic biodegradation and suggests distinct strategies for a bio-based circular plastic economy in the future (Wei et al., 2020).

We here show the complete degradation of PET, enabling a range of process optimization strategies, which is a significant advantage over lignocellulose-based processes. Lignocellulose-derived substrates come with a large fraction of solids, which are not completely degraded impeding the application of, e.g., enzyme immobilization or *in situ* removal of formed monomers (by e.g., precipitation or extraction).

While the mesophilic PET hydrolase from *I. sakaiensis* (Yoshida et al., 2016) suggests consolidated hydrolysis and utilization, we focused on

sequential plastic depolymerization and monomer conversion on purpose. This approach provides a higher flexibility for optimizing of process conditions and (bio)catalysts used. Another advantage is the built-in pasteurization step (PET hydrolysis at 70 °C), which renders the resulting solution of monomers from PET hydrolysis semi sterile. If the feedstock is for example food package waste, sterility is a huge problem.

Accessing non-biodegradable plastics of petrochemical origin (and in the future of biological origin) as carbon source for microbes enables biotechnology to valorize enormous waste streams for the sustainable production of many valuable products by exploiting the metabolic versatility of microorganisms. Products such as aromatics, organic acids, glycolipids and lipid derivatives as well as biopolymers and fuel molecules are just some examples (Tiso et al., 2016, 2017; Wynands et al., 2018; Drabo et al., 2017). More importantly, the established biosynthetic pathways for plastic monomer metabolism can also be adapted to function in different organisms, widening the applicability of the described approach even further. The production of bioplastics moreover entails the advantage that resulting products can be bio-upcycled more efficiently using the described approach as they often feature a higher biodegradability. Plastic waste biotechnological upcycling thus offers novel possibilities of end-of-life management by closing multi-million-ton material cycles in a circular economy, tackling two challenges of our petrochemical economy at the same time: Arresting the unrestrained consumption of crude oil and the resulting emission of greenhouse gases, as well as the pollution of our environment with plastic waste.

Author contributions

TT supervised the experiments regarding monomer metabolism and HAA synthesis, drafted the manuscript, and conceptualized and coordinated the study, TN provided strain *P. umsongensis* GO16, supervised the experiments regarding PHA synthesis and drafted parts of the manuscript, RW supervised the experiments regarding depolymerization and drafted parts of the manuscript, EP supervised the experiments regarding polymerization and drafted parts of the manuscript, KS carried out the experiments regarding monomer metabolism and HAA synthesis, NB carried out the experiments regarding PHA synthesis, AH carried out the experiments regarding depolymerization, MJ carried out the experiments regarding polymerization, SK was involved in PHA bioprocess design, NW was involved in conceptualizing and coordinating the study, drafted parts of the manuscript and critically read the manuscript, RP was involved in conceptualizing the study and critically read the manuscript, LA was involved in conceptualizing the study and critically read the manuscript, WZ was involved in conceptualizing the study and critically read the manuscript, KOC conceptualized the study and critically read the manuscript, LMB conceptualized and coordinated the study and critically read the manuscript. All authors read and approved the final manuscript.

Acknowledgements

The authors have received funding from the European Union's Horizon 2020 research and innovation program under grant agreement no. 633962 for the project P4SB and no. 870294 for the project MIX-UP. TN is funded by Science Foundation Ireland grant number 16/RC/3889. TT and LMB have been partially funded by the Deutsche Forschungsgemeinschaft (DFG, German Research Foundation) under Germany's Excellence Strategy – Exzellenzcluster 2186 "The Fuel Science Center" ID: 390919832. The authors thank Birger Wolter, Marie Laufens, and Franziska Faymonville for experimental support.

Appendix A. Supplementary data

Supplementary data to this article can be found online at https://doi.org/10.1016/j.ymben.2021.03.011.

References

Al-Sabagh, A.M., Yehia, F.Z., Harding, D.R.K., Eshaq, G., ElMetwally, A.E., 2016a. Fe_3O_4-boosted MWCNT as an efficient sustainable catalyst for PET glycolysis. Green Chem. 18 (14), 3997–4003.

Al-Sabagh, A.M., Yehia, F.Z., Eshaq, G., Rabie, A.M., ElMetwally, A.E., 2016b. Greener routes for recycling of polyethylene terephthalate. Egypt J. Pet. 25 (1), 53–64.

Austin, H.P., Allen, M.D., Donohoe, B.S., Rorrer, N.A., Kearns, F.L., Silveira, R.L., Pollard, B.C., Dominick, G., Duman, R., El Omari, K., Mykhaylyk, V., Wagner, A., Michener, W.E., Amore, A., Skaf, M.S., Crowley, M.F., Thorne, A.W., Johnson, C.W., Woodcock, H.L., McGeehan, J.E., Beckham, G.T., 2018. Characterization and engineering of a plastic-degrading aromatic polyesterase. Proc. Natl. Acad. Sci. U.S. A. 115 (19), E4350–E4357.

Barth, M., Oeser, T., Wei, R., Then, J., Schmidt, J., Zimmermann, W., 2015. Effect of hydrolysis products on the enzymatic degradation of polyethylene terephthalate nanoparticles by a polyester hydrolase from *Thermobifida fusca*. Biochem. Eng. J. 93, 222–228.

Barth, M., Honak, A., Oeser, T., Wei, R., Belisario-Ferrari, M.R., Then, J., Schmidt, J., Zimmermann, W., 2016. A dual enzyme system composed of a polyester hydrolase and a carboxylesterase enhances the biocatalytic degradation of polyethylene terephthalate films. Biotechnol. J. 11 (8), 1082–1087.

Bator, I., Wittgens, A., Rosenau, F., Tiso, T., Blank, L.M., 2020. Comparison of three xylose pathways in *Pseudomonas putida* KT2440 for the synthesis of valuable products. Front. Bioeng. Biotechnol. 7, 480.

Bioplastics, European, 2019. European Bioplastics Report, Bioplastics Market Development Update, 2019.

Burgard, A., Burk, M.J., Osterhout, R., Van Dien, S., Yim, H., 2016. Development of a commercial scale process for production of 1,4-butanediol from sugar. Curr. Opin. Biotechnol. 42, 118–125.

Chen, T.K., Chui, J.Y., Shieh, T.S., 1997. Glass transition behaviors of a polyurethane hard segment based on 4,4'-diisocyanatodiphenylmethane and 1,4-butanediol and the calculation of microdomain composition. Macromolecules 30 (17), 5068–5074.

Chundawat, S.P.S., Beckham, G.T., Himmel, M.E., Dale, B.E., 2011. Deconstruction of lignocellulosic biomass to fuels and chemicals. Annu. Rev. Chem. Biomol. 2, 121–145.

Covestro, A.G. [December 2019]; Available from: https://www.covestro.com/en/sustainability/lighthouse-projects/bio-anilin.

Danso, D., Schmeisser, C., Chow, J., Zimmermann, W., Wei, R., Leggewie, C., Li, X.Z., Hazen, T., Streit, W.R., 2018. New insights into the function and global distribution of polyethylene terephthalate (PET)-degrading bacteria and enzymes in marine and terrestrial metagenomes. Appl. Environ. Microbiol. 84 (8), e02773–17.

de Ilarduya, A.M., Munoz-Guerra, S., 2014. Chemical structure and microstructure of poly(alkylene terephthalate)s, their copolyesters, and their blends as studied by NMR. Macromol. Chem. Phys. 215 (22), 2138–2160.

Drabo, P., Tiso, T., Heyman, B., Sarikaya, E., Gaspar, P., Forster, J., Buchs, J., Blank, L. M., Delidovich, I., 2017. Anionic extraction for efficient recovery of biobased 2,3-butanediol - a platform for bulk and fine chemicals. ChemSusChem 10 (16), 3252–3259.

Falkenstein, P., Gräsing, D., Bielytskyi, P., Zimmermann, W., Matysik, J., Wei, R., Song, C., 2020. UV pretreatment impairs the enzymatic degradation of polyethylene terephthalate. Front. Microbiol. 11, 689.

Franden, M.A., Jayakody, L.N., Li, W.J., Wagner, N.J., Cleveland, N.S., Michener, W.E., Hauer, B., Blank, L.M., Wierckx, N., Klebensberger, J., Beckham, G.T., 2018. Engineering *Pseudomonas putida* KT2440 for efficient ethylene glycol utilization. Metab. Eng. 48, 197–207.

Germer, A., Tiso, T., Müller, C., Behrens, B., Vosse, C., Scholz, K., Froning, M., Hayen, H., Blank, L.M., 2020. Exploiting the natural diversity of the acyltransferase RhlA for the synthesis of the rhamnolipid precursor 3-(3-hydroxyalkanoyloxy)alkanoic acid. Appl. Environ. Microbiol. 86 (6), e02317–e02319.

Geyer, R., Jambeck, J.R., Law, K.L., 2017. Production, use, and fate of all plastics ever made. Sci. Adv. 3 (7), e1700782.

Guarnieri, M.T., Ann Franden, M., Johnson, C.W., Beckham, G.T., 2017. Conversion and assimilation of furfural and 5-(hydroxymethyl)furfural by *Pseudomonas putida* KT2440. Metab. Eng. Commun. 4, 22–28.

Hartmans, S., Smits, J.P., Vanderwerf, M.J., Volkering, F., Debont, J.A.M., 1989. Metabolism of styrene oxide and 2-phenylethanol in the styrene-degrading *Xanthobacter* strain 124X. Appl. Environ. Microbiol. 55 (11), 2850–2855.

Heirendt, L., Arreckx, S., Pfau, T., Mendoza, S.N., Richelle, A., Heinken, A., Haraldsdóttir, H.S., Wachowiak, J., Keating, S.M., Vlasov, V., Magnusdóttir, S., Ng, C.Y., Preciat, G., Žagare, A., Chan, S.H.J., Aurich, M.K., Clancy, C.M., Modamio, J., Sauls, J.T., Noronha, A., Bordbar, A., Cousins, B., El Assal, D.C., Valcarcel, L.V., Apaolaza, I., Ghaderi, S., Ahookhosh, M., Ben Guebila, M., Kostromins, A., Sompairac, N., Le, H.M., Ma, D., Sun, Y., Wang, L., Yurkovich, J.T., Oliveira, M.A.P., Vuong, P.T., El Assal, L.P., Kuperstein, I., Zinovyev, A., Hinton, H. S., Bryant, W.A., Aragón Artacho, F.J., Planes, F.J., Stalidzans, E., Maass, A., Vempala, S., Hucka, M., Saunders, M.A., Maranas, C.D., Lewis, N.E., Sauter, T., Palsson, B.Ø., Thiele, I., Fleming, R.M.T., 2019. Creation and analysis of biochemical constraint-based models using the COBRA Toolbox v.3.0. Nat. Protoc. 14 (3), 639–702.

Jacquin, J., Cheng, J., Odobel, C., Pandin, C., Conan, P., Pujo-Pay, M., Barbe, V., Meistertzheim, A.-L., Ghiglione, J.-F., 2019. Microbial ecotoxicology of marine plastic debris: a review on colonization and biodegradation by the "plastisphere". Front. Microbiol. 10 (865).

Jaeger, G., Magnus, J., Moussa, A.S., 2015. Production of Aniline via Anthraniliate. Covestro Deutschland AG. US20170066713A1.
Jambeck, J.R., Geyer, R., Wilcox, C., Siegler, T.R., Perryman, M., Andrady, A., Narayan, R., Law, K.L., 2015. Plastic waste inputs from land into the ocean. Science 347 (6223), 768–771.
Jehanno, C., Flores, I., Dove, A.P., Müller, A.J., Ruipérez, F., Sardon, H., 2018. Organocatalysed depolymerisation of PET in a fully sustainable cycle using thermally stable protic ionic salt. Green Chem. 20 (6), 1205–1212.
Kenny, S.T., Runic, J.N., Kaminsky, W., Woods, T., Babu, R.P., Keely, C.M., Blau, W., O'Connor, K.E., 2008. Up-cycling of PET (polyethylene terephthalate) to the biodegradable plastic PHA (polyhydroxyalkanoate). Environ. Sci. Technol. 42 (20), 7696–7701.
Kenny, S.T., Runic, J.N., Kaminsky, W., Woods, T., Babu, R.P., O'Connor, K.E., 2012. Development of a bioprocess to convert PET derived terephthalic acid and biodiesel derived glycerol to medium chain length polyhydroxyalkanoate. Appl. Microbiol. Biotechnol. 95 (3), 623–633.
Koopman, F., Wierckx, N., de Winde, J.H., Ruijssenaars, H.J., 2010. Identification and characterization of the furfural and 5-(hydroxymethyl)furfural degradation pathways of *Cupriavidus basilensis* HMF14. Proc. Natl. Acad. Sci. U.S.A. 107 (11), 4919–4924.
Lageveen, R.G., Huisman, G.W., Preusting, H., Ketelaar, P., Eggink, G., Witholt, B., 1988. Formation of polyesters by *Pseudomonas oleovorans*: effect of substrates on formation and composition of poly-(R)-3-hydroxyalkanoates and poly-(r)-3-hydroxyalkenoates. Appl. Environ. Microbiol. 54 (12), 2924–2932.
Lee, S.-C., Sze, Y.-W., Lin, C.-C., 1994. Polyurethanes synthesized from polyester polyols derived from PET waste. II. Thermal properties. J. Appl. Polym. Sci. 52 (7), 869–873.
Li, W.-J., Jayakody, L.N., Franden, M.A., Wehrmann, M., Daun, T., Hauer, B., Blank, L. M., Beckham, G.T., Klebensberger, J., Wierckx, N., 2019. Laboratory evolution reveals the metabolic and regulatory basis of ethylene glycol metabolism by *Pseudomonas putida* KT2440. Environ. Microbiol. 21 (10), 3669–3682.
Loeschcke, A., Thies, S., 2015. *Pseudomonas putida* - a versatile host for the production of natural products. Appl. Microbiol. Biotechnol. 99 (15), 6197–6214.
Ma, Y., Yao, M.D., Li, B.Z., Ding, M.Z., He, B., Chen, S., Zhou, X., Yuan, Y.J., 2018. Enhanced poly(ethylene terephthalate) hydrolase activity by protein engineering. Eng. Proc. 4 (6), 888–893.
Meyers, J., Mensah, J.B., Holzhauser, F.J., Omari, A., Blesken, C.C., Tiso, T., Palkovits, S., Blank, L.M., Pischinger, S., Palkovits, R., 2019. Electrochemical conversion of a bio-derivable hydroxy acid to a drop-in oxygenate diesel fuel. Energy Environ. Sci. 12 (8), 2406–2411.
Mückschel, B., Simon, O., Klebensberger, J., Graf, N., Rosche, B., Altenbuchner, J., Pfannstiel, J., Huber, A., Hauer, B., 2012. Ethylene glycol metabolism by *Pseudomonas putida*. Appl. Environ. Microbiol. 78 (24), 8531–8539.
Müller, R.J., Schrader, H., Profe, J., Dresler, K., Deckwer, W.D., 2005. Enzymatic degradation of poly(ethylene terephthalate): rapid hydrolyse using a hydrolase from *T. fusca*. Macromol. Rapid Commun. 26 (17), 1400–1405.
Narancic, T., Lara, MSd, Hughes, G.M., Beagan, N., Abdulmutalib, U., Kenny, S.T., Wu, H., Saccomanno, M., Um, J., O'Connor, K.E., Jimenez, J., 2021. Genome analysis of the metabolically versatile *Pseudomonas umsongensis* GO16: the genetic basis for PET monomer upcycling into polyhydroxyalkanoates. Microb. Biotechnol. 1–18.
Narancic, T., Cerrone, F., Beagan, N., O'Connor, K.E., 2020. Recent advances in bioplastics: application and biodegradation. Polymers-Basel 12 (4), 920.
Nogales, J., Gudmundsson, S., Duque, E., Ramos, J.L., Palsson, B.O., 2017. Expanding the computable reactome in *Pseudomonas putida* reveals metabolic cycles providing robustness. bioRxiv 139121.
Nogales, J., Mueller, J., Gudmundsson, S., Canalejo, F.J., Duque, E., Monk, J., Feist, A. M., Ramos, J.L., Niu, W., Palsson, B.O., 2019. High-quality genome-scale metabolic modelling of *Pseudomonas putida* highlights its broad metabolic capabilities. Environ. Microbiol. 22 (1), 255–269.
Oeser, T., Wei, R., Baumgarten, T., Billig, S., Follner, C., Zimmermann, W., 2010. High level expression of a hydrophobic poly(ethylene terephthalate)-hydrolyzing carboxylesterase from *Thermobifida fusca* KW3 in *Escherichia coli* BL21(DE3). J. Biotechnol. 146 (3), 100–104.
Olson, D.G., McBride, J.E., Joe Shaw, A., Lynd, L.R., 2012. Recent progress in consolidated bioprocessing. Curr. Opin. Biotechnol. 23 (3), 396–405.
Palm, G.J., Reisky, L., Bottcher, D., Muller, H., Michels, E.A.P., Walczak, M.C., Berndt, L., Weiss, M.S., Bornscheuer, U.T., Weber, G., 2019. Structure of the plastic-degrading *Ideonella sakaiensis* MHETase bound to a substrate. Nat. Commun. 10, 1717.
PlasticsEurope, 2018. Plastics – the Facts 2018. Available from: https://www.plasticseurope.org/application/files/6315/4510/9658/Plastics_the_facts_2018_AF_web.pdf.
Qin, J., Jiang, J., Ye, S., Wang, S., Xiao, M., Tao, Y., Jie, G., Meng, Y., 2019. High performance poly(urethane-co-amide) from CO_2-based dicarbamate: an alternative to long chain polyamide. RSC Adv. 9 (45), 26080–26090.
Rabnawaz, M., Wyman, I., Auras, R., Cheng, S., 2017. A roadmap towards green packaging: the current status and future outlook for polyesters in the packaging industry. Green Chem. 19 (20), 4737–4753.
Ragaert, K., Delva, L., Van Geem, K., 2017. Mechanical and chemical recycling of solid plastic waste. Waste Manag. 69, 24–58.
Rehm, B.H., 2010. Bacterial polymers: biosynthesis, modifications and applications. Nat. Rev. Microbiol. 8 (8), 578–592.
Ronkvist, A.M., Xie, W.C., Lu, W.H., Gross, R.A., 2009. Cutinase-catalyzed hydrolysis of poly(ethylene terephthalate). Macromolecules 42 (14), 5128–5138.
Rorrer, N.A., Nicholson, S., Carpenter, A., Biddy, M.J., Grundl, N.J., Beckham, G.T., 2019. Combining reclaimed PET with bio-based monomers enables plastics upcycling. Joule 3 (4), 1006–1027.
Rosu, D., Tudorachi, N., Rosu, L., 2010. Investigations on the thermal stability of a MDI based polyurethane elastomer. J. Anal. Appl. Pyrol. 89 (2), 152–158.
Roth, C., Wei, R., Oeser, T., Then, J., Follner, C., Zimmermann, W., Strater, N., 2014. Structural and functional studies on a thermostable polyethylene terephthalate degrading hydrolase from *Thermobifida fusca*. Appl. Microbiol. Biotechnol. 98, 7815–7823.
Salvador, M., Abdulmutalib, U., Gonzalez, J., Kim, J., Smith, A.A., Faulon, J.L., Wei, R., Zimmermann, W., Jimenez, J.I., 2019. Microbial genes for a circular and sustainable Bio-PET economy. Genes-Basel 10 (5), 373.
Scheiner, D., 1976. Determination of ammonia and Kjeldahl nitrogen by indophenol method. Water Res. 10 (1), 31–36.
Schellenberger, J., Que, R., Fleming, R.M.T., Thiele, I., Orth, J.D., Feist, A.M., Zielinski, D.C., Bordbar, A., Lewis, N.E., Rahmanian, S., Kang, J., Hyduke, D.R., Palsson, B.Ø., 2011. Quantitative prediction of cellular metabolism with constraint-based models: the COBRA Toolbox v2.0. Nat. Protoc. 6 (9), 1290–1307.
Schmidt, J., Wei, R., Oeser, T., Belisario-Ferrari, M.R., Barth, M., Then, J., Zimmermann, W., 2016. Effect of Tris, MOPS, and phosphate buffers on the hydrolysis of polyethylene terephthalate films by polyester hydrolases. Febs Open Bio 6 (9), 919–927.
Schmidt, J., Wei, R., Oeser, T., Silva, L.A.D.E., Breite, D., Schulze, A., Zimmermann, W., 2017. Degradation of polyester polyurethane by bacterial polyester hydrolases. Polymers 9 (2), 65.
Shahzadi, T., Mehmood, S., Irshad, M., Anwar, Z., Afroz, A., Zeeshan, N., Rashid, U., Sughra, K., 2014. Advances in lignocellulosic biotechnology: a brief review on lignocellulosic biomass and cellulases. Adv. Biosci. Biotechnol. 5, 246–251.
Sulaiman, S., Yamato, S., Kanaya, E., Kim, J.J., Koga, Y., Takano, K., Kanaya, S., 2012. Isolation of a novel cutinase homolog with polyethylene terephthalate-degrading activity from leaf-branch compost by using a metagenomic approach. Appl. Environ. Microbiol. 78 (5), 1556–1562.
Takeichi, T., Suefuji, K., Inoue, K., 2002. Novel poly(urethane-amide)s from polyurethane prepolymer and reactive polyamide. Preparation and properties. Polym. J. 34 (6), 455–460.
Then, J., Wei, R., Oeser, T., Gerdts, A., Schmidt, J., Barth, M., Zimmermann, W., 2016. A disulfide bridge in the calcium binding site of a polyester hydrolase increases its thermal stability and activity against polyethylene terephthalate. Febs Open Bio 6 (5), 425–432.
Tiso, T., Wierckx, N.J.P., Blank, L.M., 2015. Non-pathogenic Pseudomonas as platform for industrial biocatalysis. In: Grunwald, P. (Ed.), Industrial Biocatalysis. Pan Stanford, Singapore, pp. 323–372.
Tiso, T., Sabelhaus, P., Behrens, B., Wittgens, A., Rosenau, F., Hayen, H., Blank, L.M., 2016. Creating metabolic demand as an engineering strategy in *Pseudomonas putida* – rhamnolipid synthesis as an example. Metab. Eng. Commun. 3, 234–244.
Tiso, T., Zauter, R., Tulke, H., Leuchtle, B., Li, W.-J., Behrens, B., Wittgens, A., Rosenau, F., Hayen, H., Blank, L.M., 2017. Designer rhamnolipids by reduction of congener diversity: production and characterization. Microb. Cell Factories 16 (1), 225.
Tournier, V., Topham, C.M., Gilles, A., David, B., Folgoas, C., Moya-Leclair, E., Kamionka, E., Desrousseaux, M.L., Texier, H., Gavalda, S., Cot, M., Guémard, E., Dalibey, M., Nomme, J., Cioci, G., Barbe, S., Chateau, M., André, I., Duquesne, S., Marty, A., 2020. An engineered PET depolymerase to break down and recycle plastic bottles. Nature 580 (7802), 216–219.
Ügdüler, S., Van Geem, K.M., Roosen, M., Delbeke, E.I.P., De Meester, S., 2020. Challenges and opportunities of solvent-based additive extraction methods for plastic recycling. Waste Manag. 104, 148–182.
Walker, T.W., Frelka, N., Shen, Z., Chew, A.K., Banick, J., Grey, S., Kim, M.S., Dumesic, J. A., Van Lehn, R.C., Huber, G.W., 2020. Recycling of multilayer plastic packaging materials by solvent-targeted recovery and precipitation. Sci. Adv. 6 (47), eaba7599.
Wang, Q., Yao, X., Tang, S., Lu, X., Zhang, X., Zhang, S., 2012. Urea as an efficient and reusable catalyst for the glycolysis of poly(ethylene terephthalate) wastes and the role of hydrogen bond in this process. Green Chem. 14 (9), 2559–2566.
Wei, R., Zimmermann, W., 2017a. Biocatalysis as a green route for recycling the recalcitrant plastic polyethylene terephthalate. Microb. Biotechnol. 10 (6), 1302–1307.
Wei, R., Zimmermann, W., 2017b. Microbial enzymes for the recycling of recalcitrant petroleum-based plastics: how far are we? Microb. Biotechnol. 10 (6), 1308–1322.
Wei, R., Oeser, T., Then, J., Kuhn, N., Barth, M., Schmidt, J., Zimmermann, W., 2014a. Functional characterization and structural modeling of synthetic polyester-degrading hydrolases from *Thermomonospora curvata*. AMB Express 4 (44).
Wei, R., Oeser, T., Zimmermann, W., 2014b. Synthetic polyester-hydrolyzing enzymes from thermophilic actinomycetes. Adv. Appl. Microbiol. 89, 267–305.
Wei, R., Breite, D., Song, C., Grasing, D., Ploss, T., Hille, P., Schwerdtfeger, R., Matysik, J., Schulze, A., Zimmermann, W., 2019a. Biocatalytic degradation efficiency of postconsumer polyethylene terephthalate packaging determined by their polymer microstructures. Adv. Sci. 6 (14), 1900491.
Wei, R., Song, C., Gräsing, D., Schneider, T., Bielytskyi, P., Böttcher, D., Matysik, J., Bornscheuer, U.T., Zimmermann, W., 2019b. Conformational fitting of a flexible oligomeric substrate does not explain the enzymatic PET degradation. Nat. Commun. 10, 5581.
Wei, R., Tiso, T., Bertling, J., O'Connor, K., Blank, L.M., Bornscheuer, U.T., 2020. Possibilities and Limitations of Biotechnological Plastic Degradation and Recycling. Nat. Catal 3, 867–871 accepted.
Wierckx, N., Prieto, M.A., Pomposiello, P., de Lorenzo, V., O'Connor, K., Blank, L.M., 2015. Plastic waste as a novel substrate for industrial biotechnology. Microb. Biotechnol. 8 (6), 900–903.
Wierckx, N., Narancic, T., Eberlein, C., Wei, R., Drzyzga, O., Magnin, A., Ballerstedt, H., Kenny, S.T., Pollet, E., Avérous, L., O'Connor, K.E., Zimmermann, W., Heipieper, H.

J., Prieto, A., Jiménez, J., Blank, L.M., 2018. Plastic biodegradation: challenges and opportunities. In: Steffan, R. (Ed.), Consequences of Microbial Interactions with Hydrocarbons, Oils and Lipids: Biodegradation and Bioremediation. Springer International Publishing, Cham, pp. 1–29.

Wilkes, R.A., Aristilde, L., 2017. Degradation and metabolism of synthetic plastics and associated products by *Pseudomonas* sp.: capabilities and challenges. J. Appl. Microbiol. 123 (3), 582–593.

Wynands, B., Lenzen, C., Otto, M., Koch, F., Blank, L.M., Wierckx, N., 2018. Metabolic engineering of *Pseudomonas taiwanensis* VLB120 with minimal genomic modifications for high-yield phenol production. Metab. Eng. 47, 121–133.

Yoshida, S., Hiraga, K., Takehana, T., Taniguchi, I., Yamaji, H., Maeda, Y., Toyohara, K., Miyamoto, K., Kimura, Y., Oda, K., 2016. A bacterium that degrades and assimilates poly(ethylene terephthalate). Science 351 (6278), 1196–1199.

Zhou, L., Lu, X., Ju, Z., Liu, B., Yao, H., Xu, J., Zhou, Q., Hu, Y., Zhang, S., 2019. Alcoholysis of polyethylene terephthalate to produce dioctyl terephthalate using choline chloride-based deep eutectic solvents as efficient catalysts. Green Chem. 21 (4), 897–906.